2,7-Dichlorofluorescein Hydrazide loaded Zeolite HY: Colorimetric, Paper Strip and Fluorescent Sensor for Cu^{2+}

Sarojmoni Kalita[*] and Diganta Kumar Das

Department of Chemistry, Gauhati University, Guwahati-781014, India

*Corresponding author: E-mail: sarojmoni23@gmail.com

In this work, 2,7-dichlorofluorescein dye is successfully loaded into zeolite HY and investigated as chemosensors. The synthesized sensor was characterized by various instrumental techniques. The dye loaded sensor FH@ZHY acts as a colorimetric as well as paper strip sensor for Cu^{2+}. Fluorescence spectroscopic measurement shows that FH@ZHY exhibits high sensitivity and selectivity towards Cu^{2+} among various other metal ions in a EtOH/HEPES (1:1, v/v, pH = 7.2) solution. The behaviour of the sensor towards analyte detection was reversible with very low limit of detection. The sensing of Cu^{2+} ion by the sensor was also extended towards biological medium such as artificial cerebrospinal fluid and bovine serum albumin medium.

Keywords: Zeolite, Fluorescein, Dye loaded zeolite, Colorimetry, Fluorescent sensor, Limit of detection.

INTRODUCTION

The field of cation recognition has garnered increasing attention within the realm of analytical chemistry, owing to its significant involvement in various biological, clinical, chemical and environmental applications. In particular, heavy metal contamination has posed a serious threat to the environment due to rapid growth of industrial factories [1]. Among the heavy metals, much attention has been focused on developing sensing devices for copper ion recognition. Copper is the third most abundant divalent metal (after zinc & iron) in the human body and plays a critical role in different physiological and biological functions [2]. Copper(II) ions is a significant metal pollutant and over exposure to it causes Wilson's disease, liver or kidney damage or gastrointestinal problems [3,4]. Accumulation of excess amount of Cu^{2+} is known to cause severe diseases like Alzheimer's and Parkinson's disease [5]. Copper being a heavy metal is not biodegradable and remain stable in water and soil for a long time and slowly makes its way into the food chain eventually causing harm to humans and domestic animals [6]. Therefore, selective detection and removal of excess amount of copper is necessary for welfare of the society. Several techniques such as atomic absorption spectrometry, capillary electrophoresis, X-ray fluorescence spectrometry, inductively coupled plasma mass spectrometry have been developed [7,8]. In the recent events of development, fluorescence spectroscopy has proven to be more selective, sensitive, simple, rapid, real time monitoring with fast response of detection of heavy metal ions [9,10]. Colorimetric and paper strip sensors have also evolved as a promising method due to its rapid and concurrent on site detection, cost effectiveness and simplicity without the requirement of sophisticated instruments [11].

A large variety of fluorophores such as cyanines, pyrenes, xanthenes, coumarin, BODIPY and quinolines are utilized as chemosensors with unique properties for metal ion detection [12,13]. Among the employed fluorophores, fluorescein dye belonging to the xanthene family is one of the most commonly used probes due to its high fluorescence quantum yield and high molar extinction coefficients [14]. The spirolactam structure (closed form) of fluorescein dye opens up on interaction with specific analytes resulting in bright signals and obvious colour change and enhanced fluorescence signals [15]. The fluorescence property of fluorescein dye can also be enhanced by modifying the structure of the dye molecule [16]. However, the stability of fluorescein dye is limited and its fluorescence property can be affected due to dye aggregation or chemical degradation upon exposure to light [17]. Anchoring the dye molecules into solid matrices is known to provide resistance

against light and reacting agents along with improving its spectral properties. There are a variety of solid supports employed for anchoring fluorescein dye molecules like dextrines, polymers, porous silica, mesoporous materials and zeolites [18].

With recent advances in nanotechnology and material science, the development of microporous materials as host is the key to develop highly sensitive and selective optical chemical sensors. In recent years, solid hosts like zeolites have garnered much attention owing to its excellent ion exchange capacity, chemical and thermal stability and low cost of extraction [19]. Zeolites are hydrated aluminosilicates of the tectosilicates family, where the SiO_4 tetrahedra form 3D super cages. In their structure, some Al atoms substitute Si atoms resulting in a negatively charged structure which originates from the difference in SiO_4^{4-} and AlO_4^{4-} tetrahedral. Due to their rigid 3D network, zeolites exhibit excellent well defined structural properties, thermal stability, uniform channels, shape and charge selectivity, low cost and resistance to extreme chemical conditions. These properties are highly ideal for obtaining organized arrangements for a wide variety of dye molecules [20]. Pellejero *et al.* [21] reported an optochemical humidity sensor based on immobilization of Nile red dye into zeolite HY. In another report, Viboonratanasari *et al.* [22] developed a rhodamine 6G dye loaded HY zeolite for selective detection of nitrite ion. Recently, Bertao *et al.* [23] reported the modification of paper based devices with dye nanomaterials encapsulated in Y and ZSM-5 zeolites. A Pb^{2+} sensor was developed by encapsulating carbon dots in zeolite imidazole framework [24].

In this work, 2,7-dichlorofluorescein hydrazide dye has been incorporated into zeolite HY as fluorescent probe. The synthesized probe showed fluorescent enhancement behaviour towards Cu^{2+} ion in EtOH:HEPES (1:1, v/v) solution. It also acts as a selective colorimetric and paper strip sensor for Cu^{2+} ion. The detection of Cu^{2+} ion by the sensor is selective, sensitive and reversible with low detection limits. The sensing of the analyte was also carried out in biological medium like artificial cerebrospinal fluid (ACF) and bovine serum albumin (BSA) medium.

EXPERIMENTAL

All the chemicals are purchased either from Sigma-Aldrich or LOBA. The metal salts except for $Pb(NO_3)_2$, $CdCl_2$ and $HgCl_2$ were sulphates. The chemicals were of analytical grade and used without further purification. The chemical solutions (10^{-4} M) were prepared in deionized water obtained from quartz double distilled plant. The FT-IR spectra were recorded in a Perkin-Elmer RXI spectrometer as KBr pellets. The fluorescence and UV-visible spectra were recorded in HITACHI 2500 and Shimadzu UV 1800 spectrophotometer, respectively using quartz cuvette (1 cm path length). Scanning electron microscopy was done using Zeiss FESEM Sigma 300 and energy dispersive X-ray spectroscopy was studied using Ametek EDAX. The diffuse reflectance spectra of the samples were recorded in a HITACHI, U-4100 spectrophotometer. Thermogravimetric analysis (TGA) was done using Metter Toledo TGA/DSC1 STAR^e system in presence of nitrogen atmosphere in the temperature range 50-700 °C at a heating rate of 10 °C/min. Powder X-ray diffraction (PXRD) patterns of the synthesized samples were recorded using a Rigaku Ultima IV X-ray diffractometer (Cu$K\alpha$ radiation, $\lambda = 1.5418$ Å) at 40 kV and 40 mA. High resolution mass spectrometry of the sample was recorded using Xevo G2-XS QTOF (Waters).

Preparation of H-type zeolite Y: The sodium form of zeolite was converted into its H-form by the ammonium ion exchange method [25]. Zeolite NaY (1 g) was treated with 100 mL of 1 M NH_4Cl solution at 80 °C for 2 h. The resulting mixture was filtered and washed with deionized water and then the sample was oven dried at 120 °C for 5 h. The cycle was repeated for three times to get a complete exchange of sodium. In the final step, the sample was heated at 550 °C for 5 h to decompose to H-form of zeolite Y.

Synthesis of 2,7-dichlorofluorescein hydrazide (FH): 2,7-Dicholorofluorescein (0.3 g) was dissolved in 20 mL ethanol and an excessive hydrazine hydrate (1.2 mL) was added. The reaction solution was refluxed in oil bath for 5 h with continuous stirring. After cooling the solution at room temperature, solvent was evaporated and the residue was recrystallized using methanol [26] (**Scheme-I**).

The FT-IR spectrum of FH was recorded in KBr pellet (Fig. 1a) and the bands observed were at 3700-3600 cm^{-1} (N-H *str.*), 3500 cm^{-1} (O-H *str.*), 1680 cm^{-1} (C=O *str.*), 1170 (C-N *str.*), 1600 and 1452 cm^{-1} (C-C *str.* aromatic ring) and 1065 cm^{-1} (C-H *bend.*). The HRMS spectrum of FH (Fig. 1b) exhibited a strong molecular peak at *m/z* value: [M+H] calculated for $C_{20}H_{12}Cl_2N_2O_4$ is 415.03, found 415.027.

Preparation of sensor FH@ZHY: Using the method described by Neves *et al.* [27], the synthesized FH dye was loaded into the zeolite HY, a 3D network with a pore size of about 7.5 Å. Dye (0.05 g) was dissolved in 50 mL ethanol and
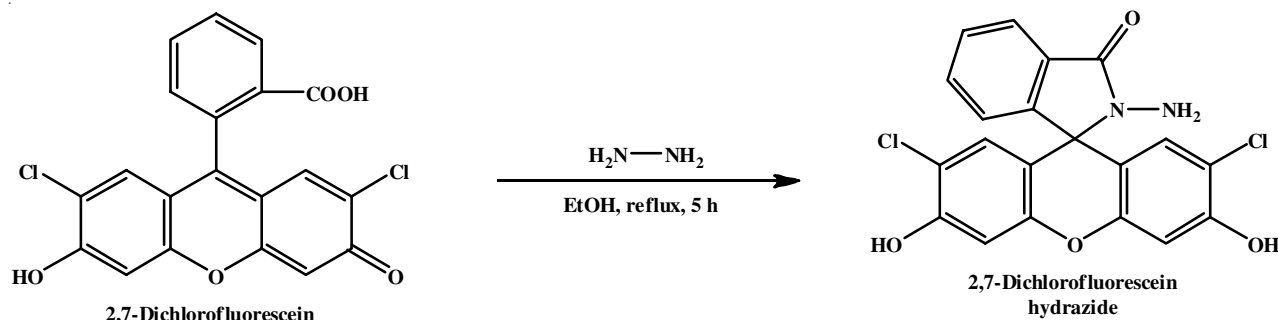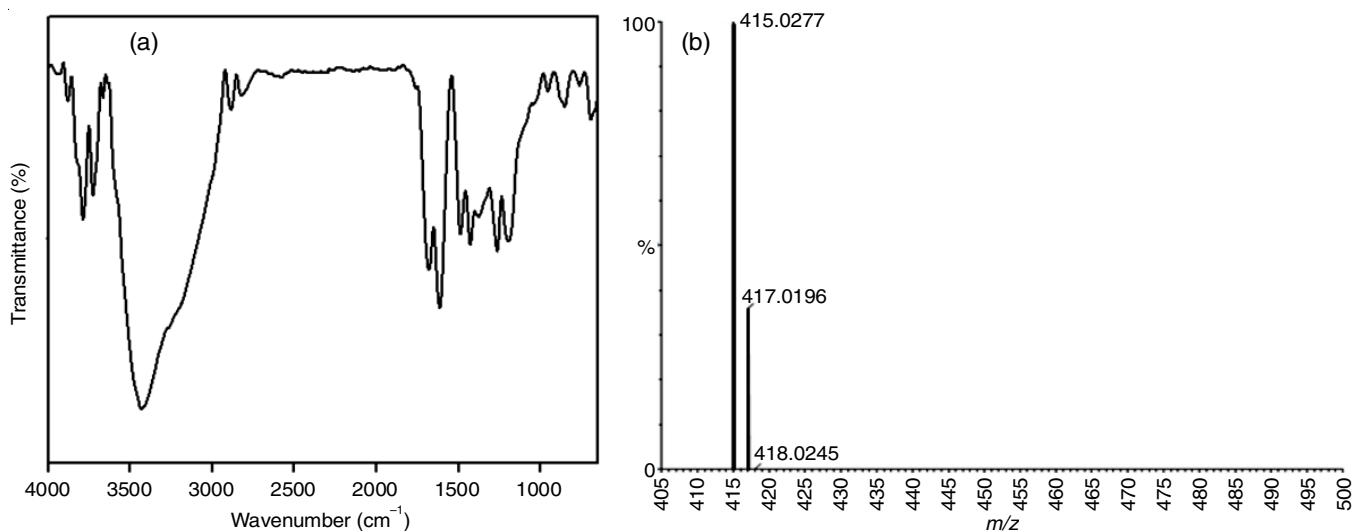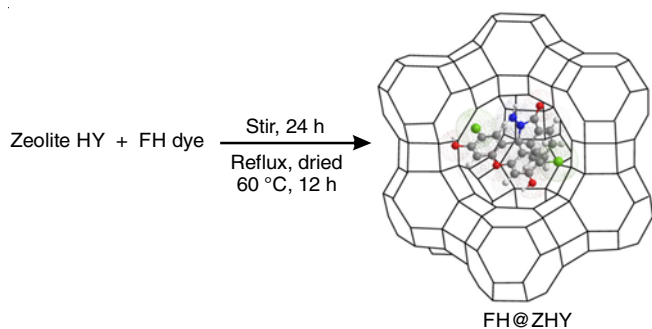

Scheme-I: Synthesis of FH dye

Fig. 1. (a) FTIR and (b) HRMS spectrum of FH

then 1 g of zeolite HY was added to the solution. The mixture was stirred for 48 h at room temperature and the resulting suspension was filtered, washed with ethanol and dried at 80 ºC for 10 h (**Scheme-II**). The sample was then subjected to Soxhlet extraction for 8 h in 100 mL ethanol. Finally, the sample was dried at 60 ºC for 12 h and the prepared sensor is designated as FH@ZHY.

Scheme-II: Preparation route of FH@ZHY

Synthesis of artificial cerebrospinal fluid (ACF): ACF containing majority of the interfereents in the real cerebrospinal fluid was prepared by the reported method [28], In brief, 2.1 g NaCl, 0.07 g KCl, 0.08 g $CaCl_2$, 0.2 g glucose, 0.4 g $NaHCO_3$ and 0.002 g urea were mixed together in a 250 mL volumetric flask. The pH of the solution was maintained at 7.4 with the help of HEPES buffer. The solution was immediately used to avoid the hydrolysis of urea.

RESULTS AND DISCUSSION

Infrared studies: In the IR spectrum of zeolite NaY and HY (Fig. 2), strong band centered at 3500 cm^{-1} is due to surface hydroxyl and O-H of lattice water. The FT-IR spectra of zeolite NaY and HY were matched well with each other except some differences in the intensity of peaks in the region 3600-3400 cm^{-1}. The peak for hydroxyl group in zeolite HY is more intense and sharp due to its stronger Brønsted acid property [29]. A sharp peak at 1074 cm^{-1} is due to skeletal vibration of Si(Al)-O
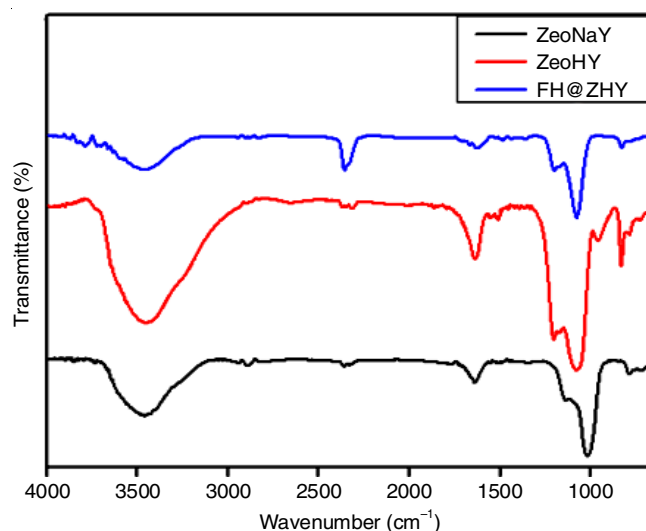

Fig. 2. FT-IR spectra of ZNaY (black line), ZHY (red line) and FH@ZHY (blue line)

bonds in the tetrahedral groups of HY zeolite. The structural peaks in the region 900-600 cm^{-1} are assigned to the vibrations of T-O-T, O-T-O and T-O bonds in the tetrahedral SiO_4 and AlO_4 units. The dye loaded composite mainly maintains the typical strong bands of the host structure. Moreover, the extraction of dye loaded sample with ethanol resulted in considerable decrease in band intensity.

XRD studies: Fig. 3 shows the powder XRD pattern of the respective samples recorded at 2θ values between 5º and 50º. The HY form of zeolite maintained the same diffraction pattern as highly crystalline NaY form of zeolite, while some of the peaks intensity were narrowed. The appearance of peaks is assigned to (111), (331), (511), (440), (533), (555) and (642) reflections [30]. After dye loading, the intensity of XRD peaks was further reduced and the dye loaded composite exhibited the characteristics peaks of the host zeolites. The reduced intensity after dye loading might be due to dispersion of the dye molecules on the surface of solid support in the form of a monolayer [31].
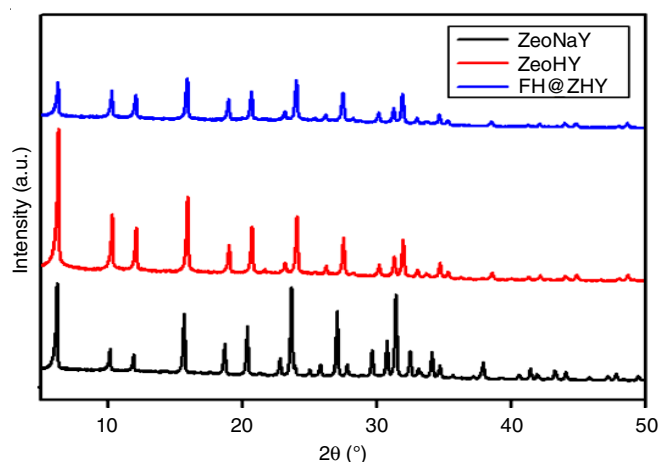
Fig. 3. PXRD pattern of ZNaY (black line), ZHY (red line) and FH@ZHY (blue line)

Morphological studies: In order to analyze the surface morphology, particle distribution and elemental compositions, SEM-EDX analysis was performed (Fig. 4). The crystallites of zeolite NaY and HY exhibited a well defined octahedral shape in the size range of 0.8-1 µm. After loading of the dye, some portion of the crystallites of zeolite is covered with the dye molecules, but most of the dye is removed after washing. The dye adsorbed surface exhibited roughness and distortion from the regular shape of HY zeolite. Nevertheless, the dye molecules partially protruding from zeolite grain can facilitate sticking of the crystallites.

Thermal decomposition: The TGA plot of zeolite NaY, zeolite HY and the sensor FH@ZHY is shown in Fig. 5. In case of zeolite NaY and HY, the major weight loss occurred at around 100 ºC due to dehydration and desorption of remnants of alcohol used during the extraction process [32]. The dye
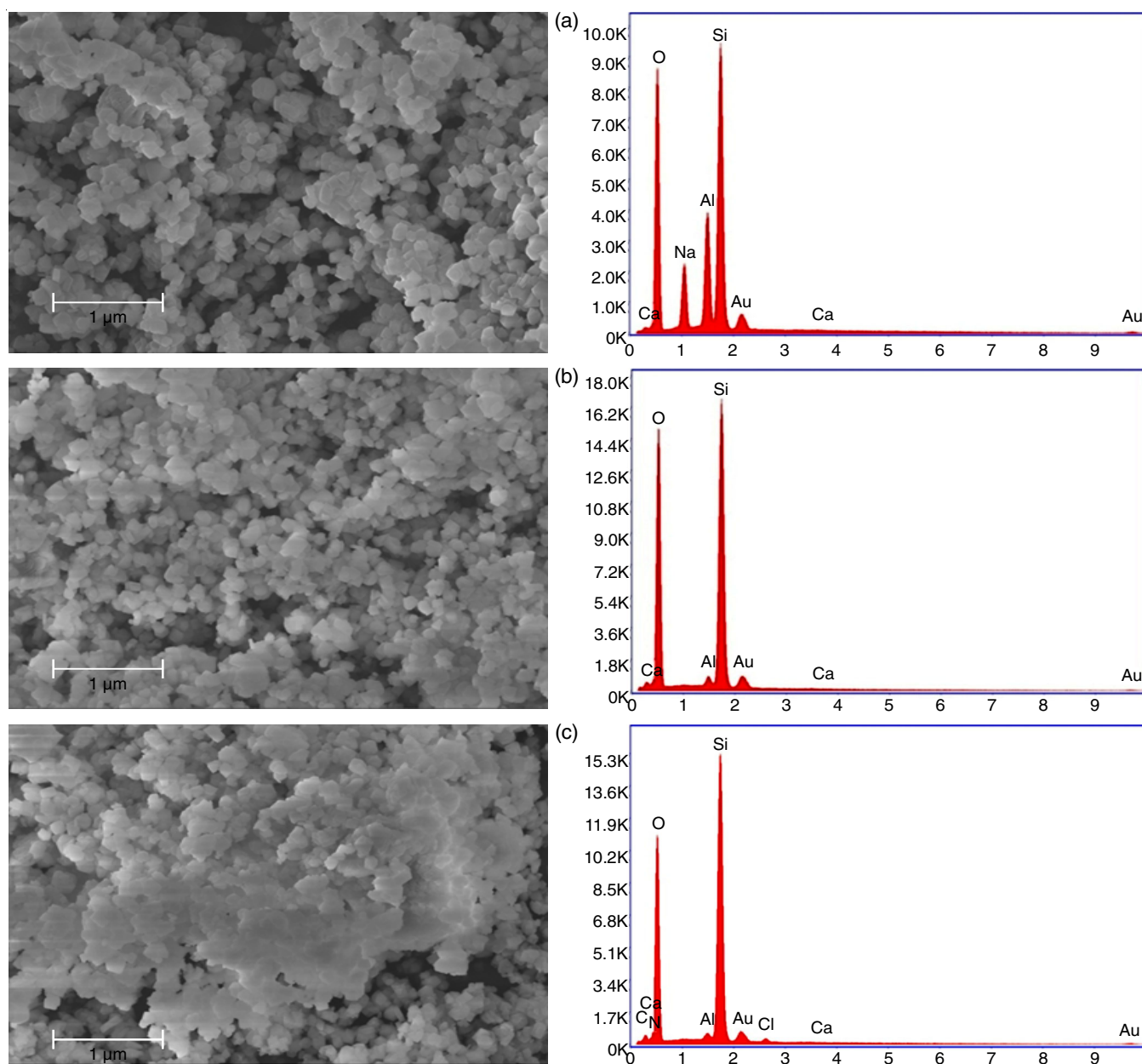

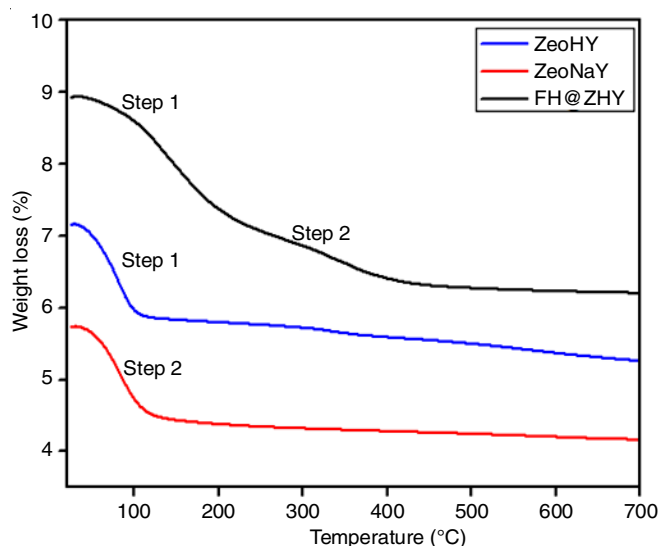Fig. 4. SEM and EDX analysis of (a) ZNaY (b) ZHY and (c) FH@ZHY

Fig. 5. TGA data of ZNaY, ZHY and FH@ZHY

loaded zeolite HY undergoes two step weight losses. The first weight loss at 110 ºC is due to loss of physisorbed water molecules. The second weight loss in the range 300-500 ºC is due to decomposition and combustion of organic moieties of the dye molecule.

UV-VIS/diffuse reflectance spectra: The diffuse reflectance spectra of zeolite NaY, HY, FH dye and FH@ZHY are shown in Fig. 6. The sensor FH@ZHY exhibits bands at 285 nm
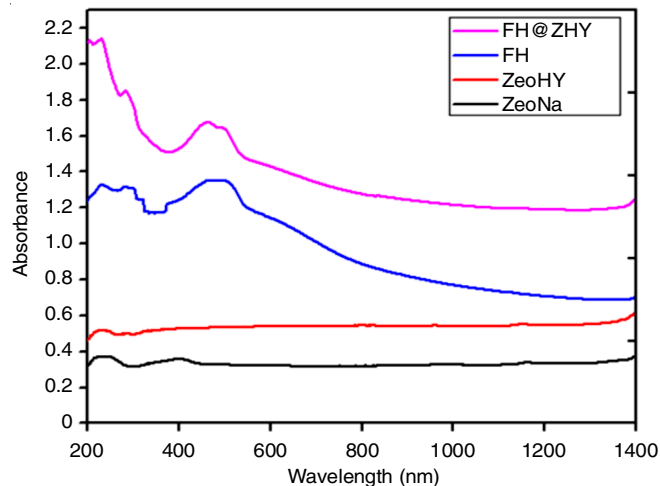

Fig. 6. UV-DRS spectra

and 466 nm and these bands are broadened and slightly blue shifted compared to the pristine FH dye (493 nm). This blue shift can be attributed to the aggregates of the dye surrounding the zeolite crystallites.

FH@ZHY as colorimetric and paper strip sensor for Cu²⁺: Colorimetric sensing of Cu²⁺ was done under normal light as well as under 365 nm UV radiation lamp. The colour of the stock solution of FH@ZHY containing Cu²⁺ turned yellowish, which is visible to naked eye. The solution of the sensor containing Cu²⁺ was also observed under UV lamp. Fig. 7 shows the generation of green fluorescence for the solution with Cu²⁺ ion solution. The solution containing other metal ions did not impart any colour to the sensor solution except Cu²⁺ (Fig. 8). Paper strip detection for FH@ZHY in presence of Cu²⁺ was also studied. For this purpose, Whatman filter paper was cut into small strips. Each strip was wetted with the solution of the sensor using a micropipette and allowed to dry. Different metal solutions (10 μL) were added to the paper strip and allowed to dry. This process was repeated for three times. From Fig. 9, it is clear that only the strip impregnated with Cu²⁺ developed a yellowish colour under normal light while the other metal ions did not show any characteristic development of colour to the paper strips.
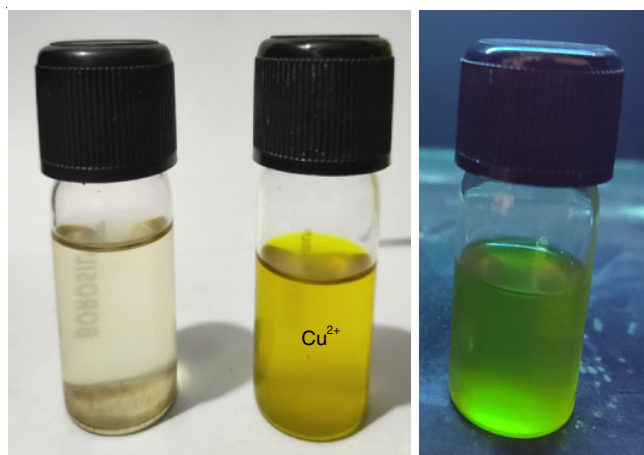
Fig. 7.   Development of colour for FH@ZHY in ethanol in presence of Cu²⁺ under normal light (left image) and UV lamp (right image)

FH@ZHY as fluorescent sensor for Cu²⁺: The fluorescence spectrum of FH@ZHY was recorded by exciting it with 480 nm of photons with 5 nm slit for both excitation and
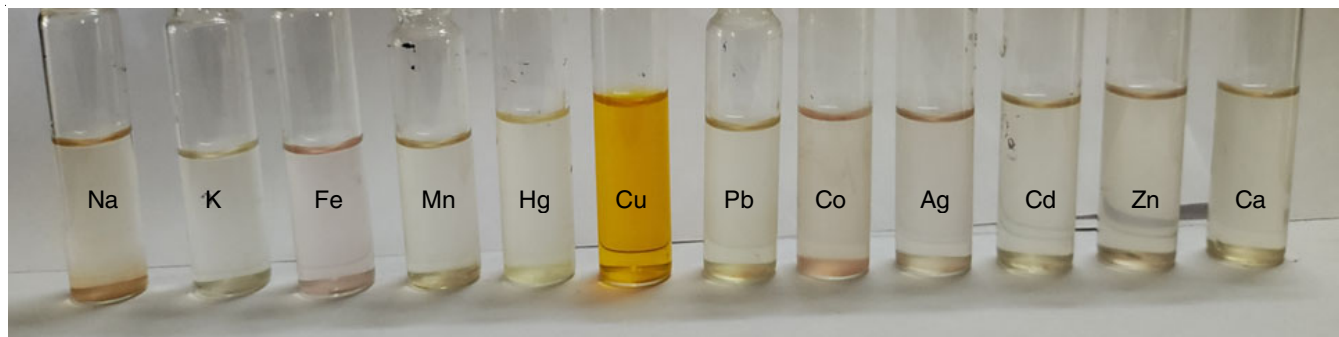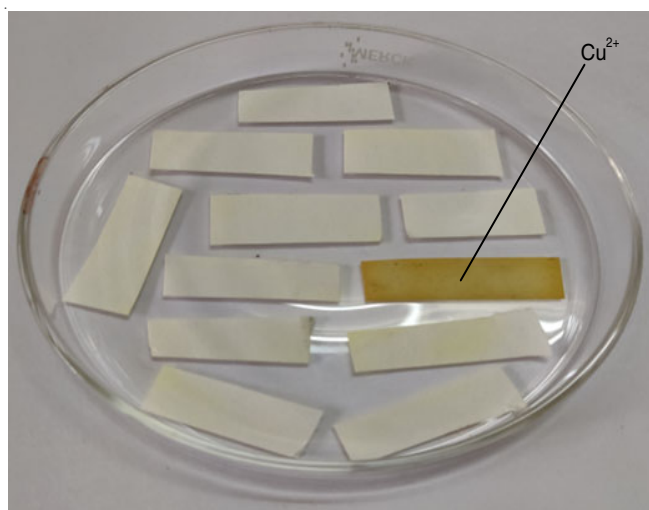

Fig. 8. Colour Change of FH@ZHY on addition of different metal ions
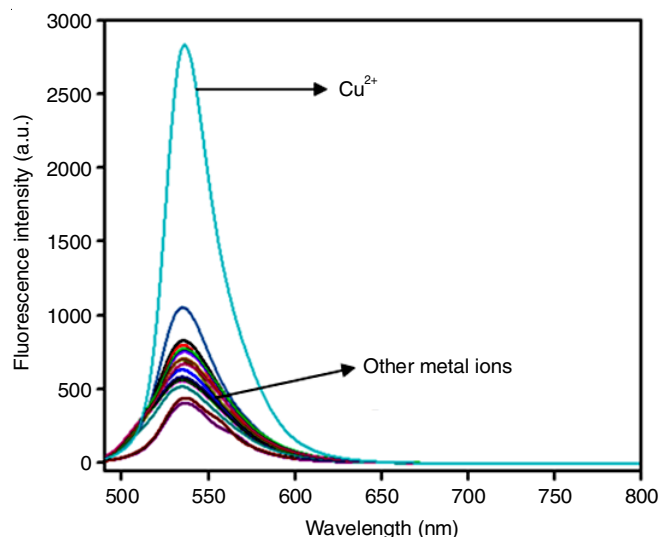
Fig. 9. Paper strip sensor for Cu^{2+}

Fig. 10. Fluorescence plot of FH@ZHY in EtOH:HEPES (1:1, v/v, pH = 7.2) in presence of different metal ions

emission. The fluorescent spectrum of the sensor shows a peak at 535.2 nm with peak intensity *ca.* 500. To this solution, 50 µL of different metal ions were added one at a time and its spectrum was recorded. Fig. 10 shows the fluorescent plot of FH@ZHY in presence of different metal ions. As evident from the plot, peak intensity is enhanced only in case of Cu^{2+} ion. Fig. 11 compares the I/I_o values of the sensor in presence of different metal ions, where I_o is the fluorescence intensity of the sensor in absence of metal ions and I is the fluorescence intensity in presence of an equivalent of different metal ions. After the recognition study, fluorescence titration was carried out for different added concentration of Cu^{2+} to the sensor solution. The concentration of Cu^{2+} inside the cuvette increased from 0.49×10^{-7} M to 6.5×10^{-7} M upon addition of 10-140 µL metal solution. As indicated in Fig. 12a, the fluorescent peak intensity at 535 nm increases upon the analyte addition. The increment in peak intensity of FH@ZHY by Cu^{2+} is almost 13 times to that of the original. The plot of fluorescence intensity *vs.* analyte concentration fits linearly with $R^2 = 0.993$ (Fig. 12b).
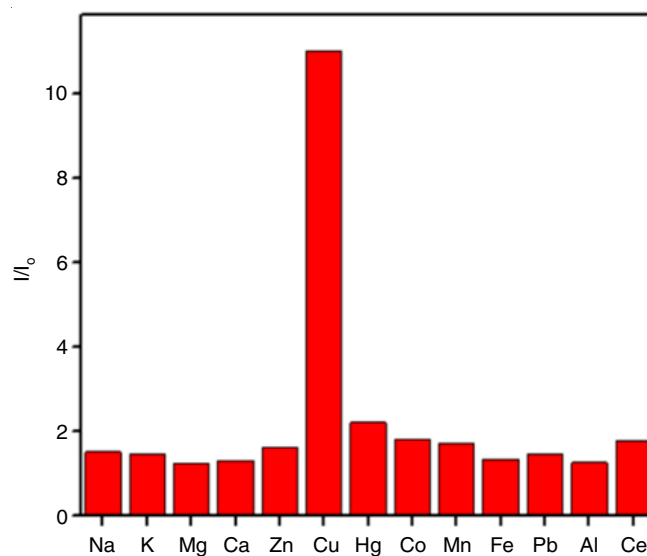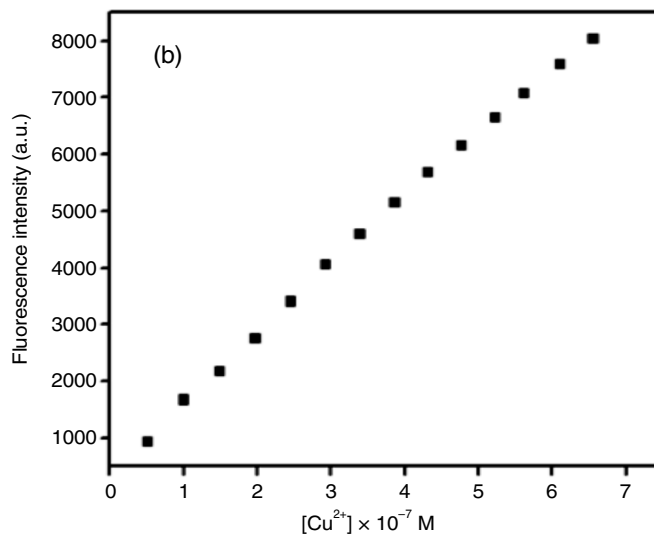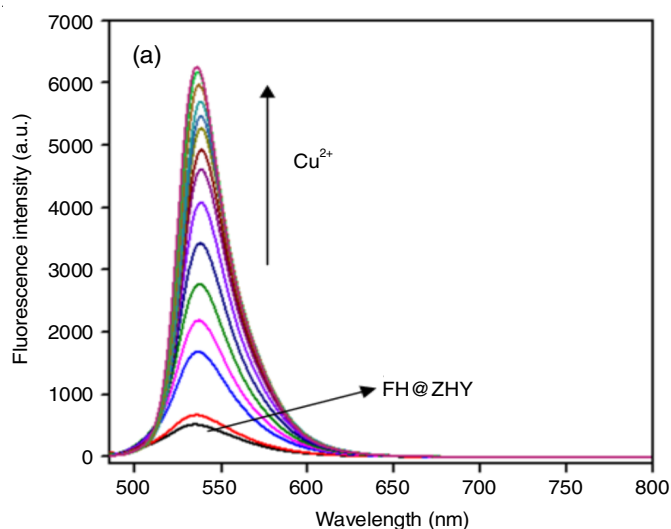

Fig. 11. I/I_o value of various metal ions

Fig. 12. (a) FL plot of FH@ZHY in EtOH:HEPES upon gradual addition of Cu^{2+} ion, (b) plot of FL intensity *vs.* $[Cu^{2+}]$
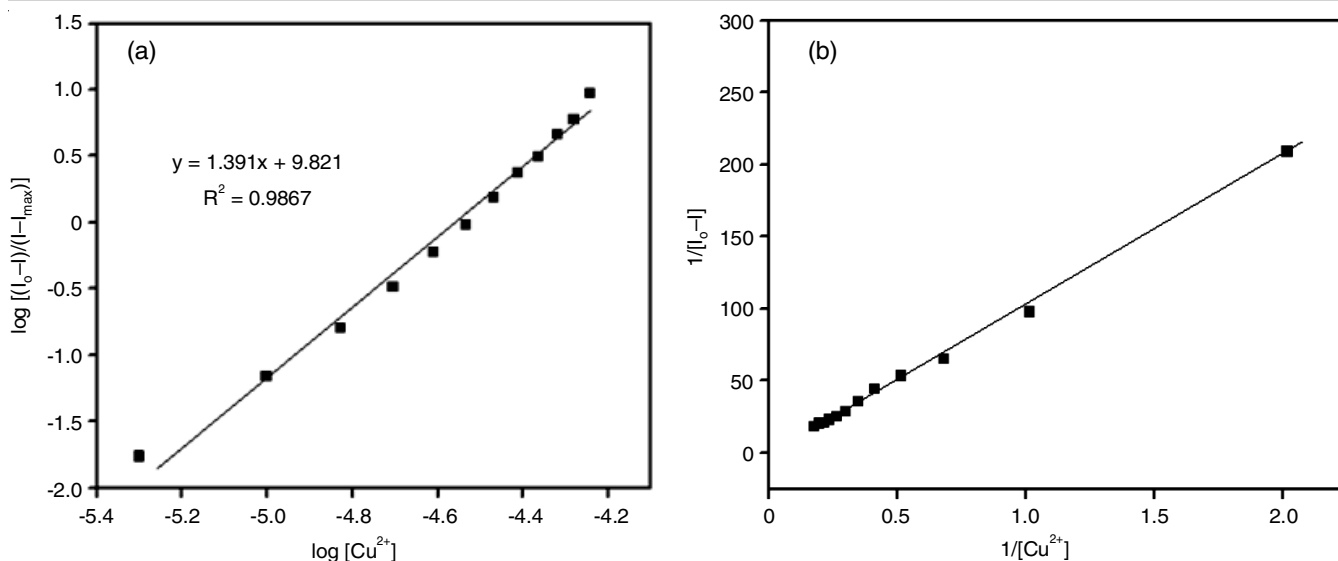
Fig. 13. (a) Plot of log $[(I_o-I)/(I-I_{max})]$ *versus* log $[Cu^{2+}]$, (b) Benesi-Hildebrand plot of FH@ZHY for Cu^{2+}

The stoichiometry of binding was determined from the plot of log $[(I_o-I)/(I-I_{max})]$ as a function of $[Cu^{2+}]$ (Fig. 13a), where I_o is the fluorescence intensity of FH@ZHY in absence of Cu^{2+}; I is the fluorescence intensity of FH@ZHY at different added concentrations of Cu^{2+} and I_{max} is the highest intensity of FH@ZHY upon titration with Cu^{2+} ion solution. The slope was found to be 1.391, which is an indication of 1:1 interaction between FH@ZHY and Cu^{2+}. The binding stoichiometric constant (K_a) was derived using the Benesi-Hildebrand equation (Fig. 13b). The detection limit (LOD) of the sensor towards Cu^{2+} has been determined as per standard deviation method. The LOD was calculated employing the equation: $3\sigma/K$ [33], where σ is the standard deviation of the blank sensor solution and K is the slope obtained from the plot of fluorescence intensity *vs.* Cu^{2+} concentration. The limit of detection and binding constant (K_a) is given in Table-1.

TABLE-1
LOD AND K_a VALUE OF FH@ZHY FOR Cu^{2+}

Sensor LOD	K_a
FH@ZHY 2.5×10^{-10} M	5.37×10^7 M⁻¹

UV-visible studies: Fig. 14 shows the UV-visible spectral change of FH@ZHY upon the gradual addition of Cu^{2+} ion in ethanol. Upon addition of Cu^{2+} ion to the sensor solution, peak intensity at 290 nm increases with slight blue shift in absorbance peak upon gradual increase in concentration of the analyte. The plot of absorbance *vs.* $[Cu^{2+}]$ indicates a linear change with increasing concentration of the analyte (Fig. 15a). The binding stoichiometric ratio between the sensor and analyte is calculated from the plot of log $[(A_o-A)/(A-A_{max})]$ *vs.* log $[Cu^{2+}]$ (Fig. 15b), where A_o is the absorbance of FH@ZHY in absence Cu^{2+}, A is the absorbance of FH@ZHY at different added concentration of Cu^{2+} and A_{max} is the highest absorbance value of FH@ZHY on adding one equivalent of Cu^{2+}. The slope of 1.263, which confirms 1:1 binding between FH@ZHY and Cu^{2+}. The value obtained is similar to that obtained from the fluorescence data.
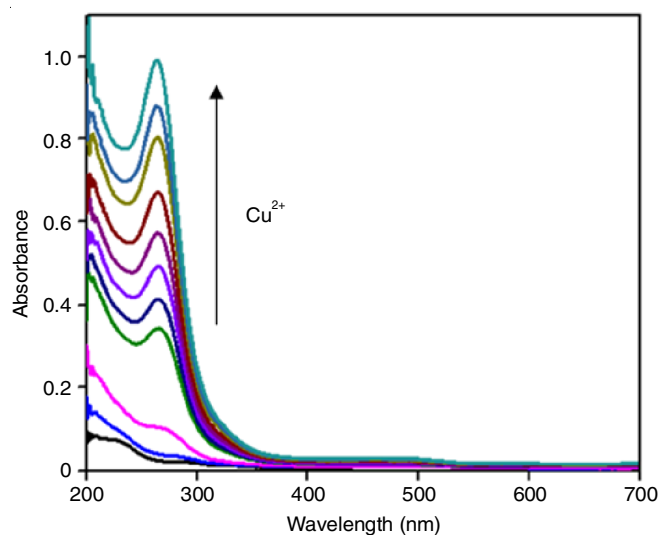

Fig. 14. UV-Vis plot of FH@ZHY upon Cu^{2+} addition in EtOH:HEPES (1:1, v/v, pH = 7.2)

Interference study: The interference possibilities by other metal ions on the selective and sensitive detection of Cu^{2+} by the sensor were studied. For this purpose, one equivalent of different metal ions (Na^+, K^+, Zn^{2+}, Co^{2+}, Mn^{2+}, Mg^{2+}, Fe^{3+}, Pb^{2+}, Ce^{3+}, Ca^{2+}, Hg^{2+}, Al^{3+}) was added to the sensor solution followed by addition of one equivalent of Cu^{2+}. Fig. 16 shows that Cu^{2+} could enhance the fluorescence intensity of FH@ZHY in presence of other metal ions to the same extent it did in absence of other metal ions.

Reversibility studies: The reversibility of binding of FH@ZHY towards Cu^{2+} ion has been checked with the metal ion chelator, Na_2EDTA. A 50 μL of Cu^{2+} was added to solution of FH@ZHY in ethanol in quartz cuvette and allowed to stand for 10 min. The fluorescence spectrum was recorded for same. To a solution containing Cu^{2+}:FH@ZHY, $EDTA^{2-}$ (10^{-3} M) was gradually added. The fluorescence intensity was found to decrease with the addition of $EDTA^{2-}$ (Fig. 17), which confirms that the binding of analyte to the sensor is reversible in nature.
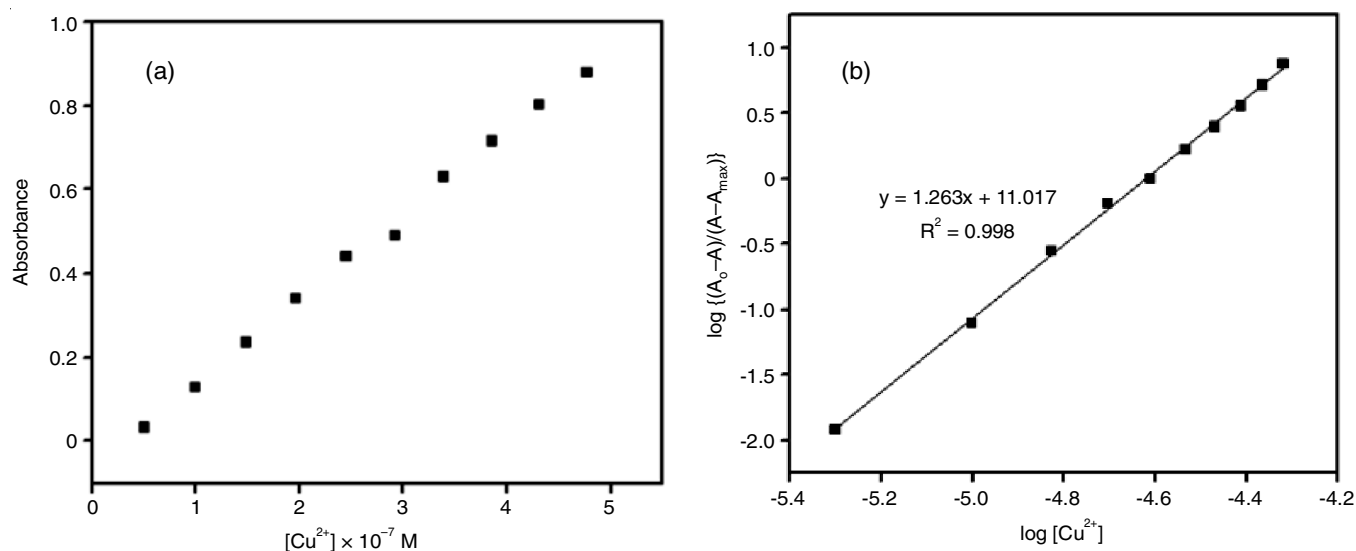
Fig. 15. (a) Calibration plot of absorbance *vs.* $[Cu^{2+}]$ and (b) plot of log $[(A_o-A)/(A-A_{max})]$ *vs.* log $[Cu^{2+}]$
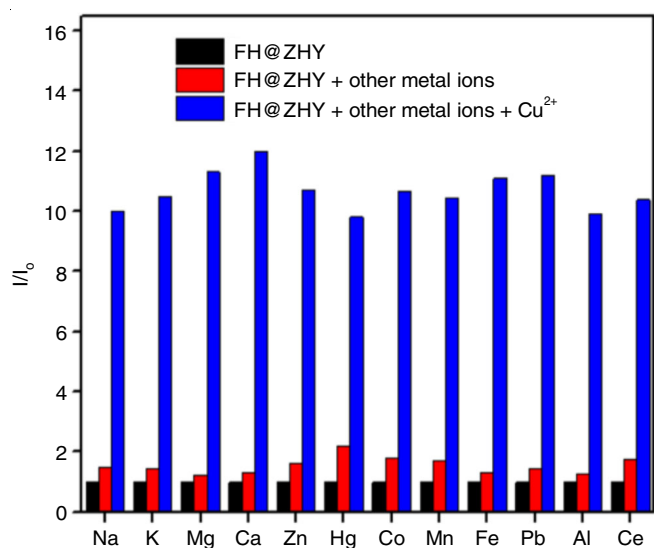

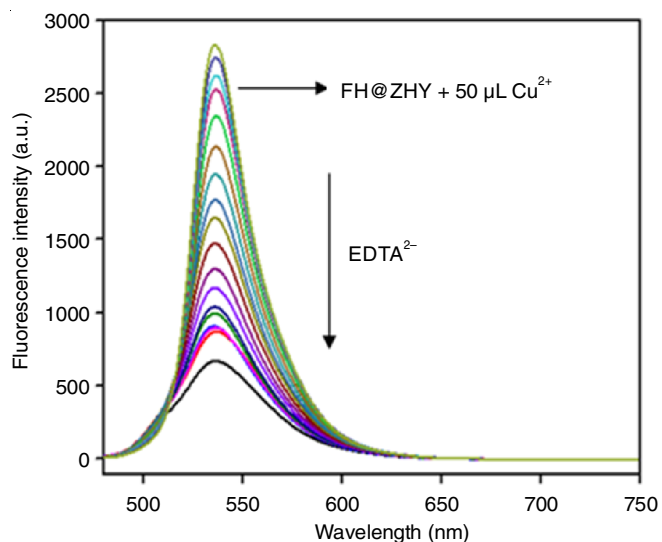Fig. 16. Metal interference study of FH@ZHY in presence of various competing metal ions

Fig. 17. Plot of reversible behaviour

Proposed mechanism of binding: In order to gain insight into the sensing mechanism of Cu^{2+}, it is most related to the change in structure between spirocyclic and opencyclic forms. The hypothesized mechanism of Cu^{2+} binding to the sensor is shown in **Scheme-III**. In absence of metal ion, the sensor remains in the spirocyclic form which is colourless and non-fluorescent. Upon addition of Cu^{2+}, it coordinates with the heteroatoms of the sensor. This complexation leads to obvious colour change and results in strong absorption spectrum. The complexation with Cu^{2+} further induces the hydrolytic cleavage of N=C bond which opens the spirocycle. This spirolactam ring opening is responsible for the colour change and appearance of strong green fluorescence under UV lamp and further fluorescence emission spectra at 535 nm.

Biological applications

Detection of Cu^{2+} in bovine serum albumin (BSA): For the detection of Cu^{2+} in BSA medium, 1 mL BSA solution (HEPES buffer, pH = 7.4) was added to 5 mL sensor solution and kept on standing for 30 min. The spiked solution was then used for fluorescence spectral titration for detection of Cu^{2+} metal ion. Fig. 18a shows fluorescence peak enhancement of FH@ZHY at 535 nm upon addition of Cu^{2+} ion to the spiked solution. The fluorescence enhancement is about 11 times upon the analyte addition to sensor solution in BSA medium. The relationship between fluorescence intensity and Cu^{2+} concentration exhibits a linear correlation within a specific range of 0.49×10^{-7} M to 6.5×10^{-7} M. The LOD was also calculated for the sensor towards Cu^{2+} in BSA medium and found to be 0.78×10^{-10} M.

Detection of Cu^{2+} in artificial cerebrospinal fluid (ACF): The determination of Cu^{2+} in ACF medium was carried out to evaluate the selectivity and sensitivity of the sensor FH@ZHY towards Cu^{2+} detection. For this purpose, 5 mL solution of FH@ZHY in EtOH:HEPES (pH = 7.4) was spiked with 0.5 mL solution of freshly prepared ACF. The spiked solution was then titrated against different concentrations of Cu^{2+}. An enhancement of fluorescence intensity at 535 nm was thereby observed
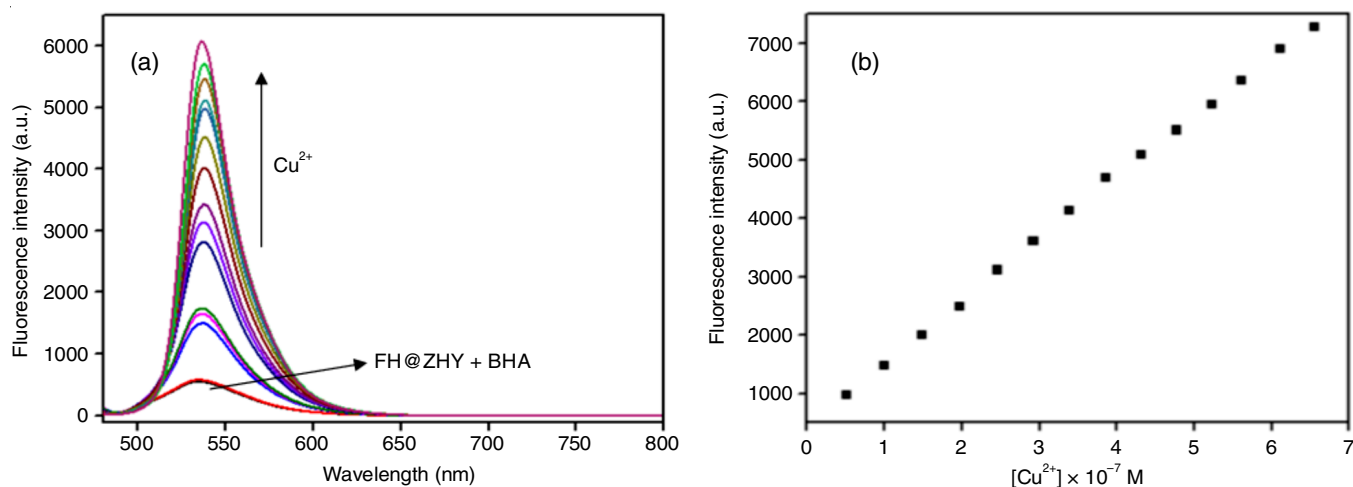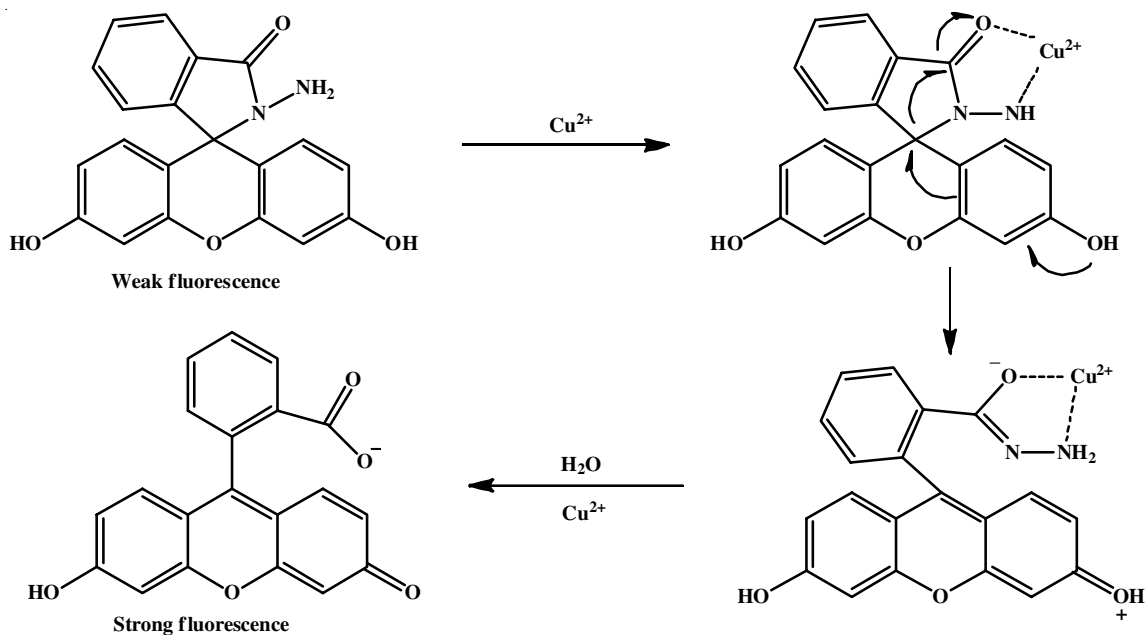
Scheme-III: Proposed mechanism of sensing

Fig. 18. (a) Fluorescence plot of FH@ZHY in BSA medium (pH = 7.4) upon addition of Cu²⁺, (b) calibration plot of fluorescence intensity *vs.* [Cu²⁺]
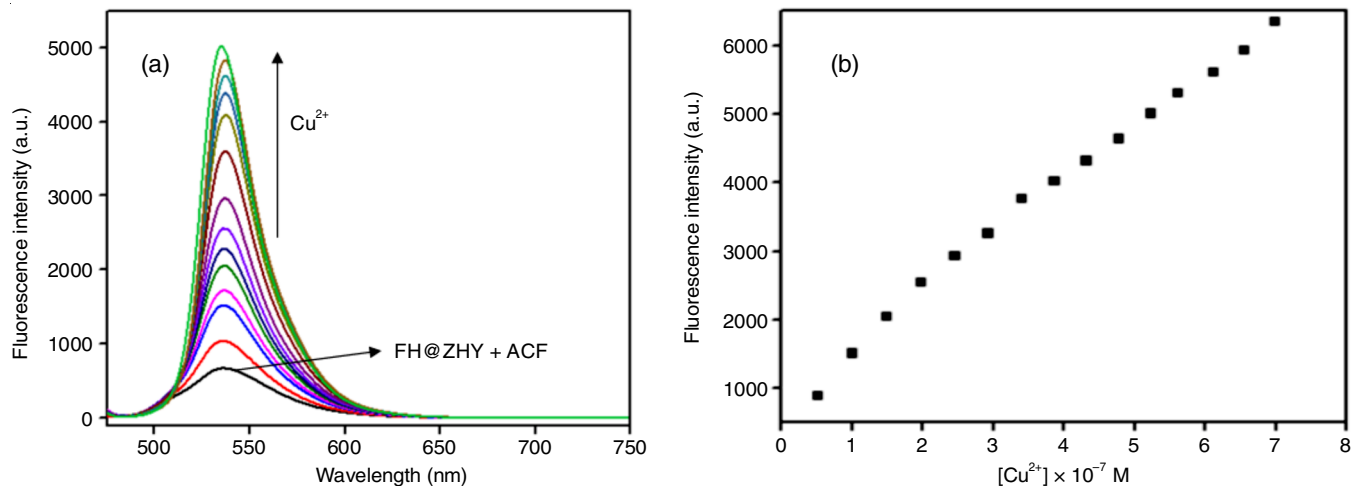

Fig. 19. (a) Fluorescence plot of FH@ZHY in ACF medium (pH = 7.4) upon addition of Cu²⁺, (b) calibration plot of fluorescence intensity *vs.* [Cu²⁺]

which suggests the successful detection of Cu^{2+} in ACF medium (Fig. 19a). An increment in intensity was about 10 times with a linear range of 0.49×10^{-7} M to 7×10^{-7} M (Fig. 19b). The LOD in synthetic ACF medium was calculated to be 0.87×10^{-10} M.

Conclusion

2,7-Dichlorofluorescein dye is successfully loaded into zeolite HY (FH@ZHY) was successfully prepared and applied as chemosensor. The sensor was characterized by various instrumental techniques like FT-IR, PXRD, SEM-EDX analysis, TGA and UV-DRS spectroscopy. The sensor FH@ZHY acts as colori-metric and paper strip sensor to selectively detect Cu^{2+} ion. Moreover, the sensor FH@ZHY could also detect Cu^{2+} by turn-on fluorescence spectroscopic method. The detection was selective, sensitive and reversible with very low detection limits. The probable mode of sensing can be attributed to the spiro-lactam ring opening of the dye part of the sensor upon analyte addition. The sensor could also successfully detect Cu^{2+} ion in the artificial cerebrospinal fluid and bovine serum albumin medium.

CONFLICT OF INTEREST

The authors declare that there is no conflict of interests regarding the publication of this article.

REFERENCES

1. M.R. Saidur, A.R. Aziz and W.J. Basirun, *Biosens. Bioelectron.*, **90**, 125 (2017);
   https://doi.org/10.1016/j.bios.2016.11.039
2. R. Martínez-Máñez and F. Sancenón, *Chem. Rev.*, **11**, 4419 (2003);
   https://doi.org/10.1021/cr010421e
3. L. Tang, P. He, K. Zhong, S. Hou and Y. Bian, *Spectrochim. Acta A Mol. Biomol. Spectrosc.*, **169**, 246 (2016);
   https://doi.org/10.1016/j.saa.2016.06.045
4. H. Tapiero, D.M. Townsend and K.D. Tew, *Biomed. Pharmacother.*, **57**, 386 (2003);
   https://doi.org/10.1016/S0753-3322(03)00012-X
5. J.S. Valentine and P.J. Hart, *Proc. Natl. Acad. Sci. USA*, **100**, 3617 (2003);
   https://doi.org/10.1073/pnas.0730423100
6. K.J. Barnham, C.L. Masters and A.I. Bush, *Nat. Rev. Drug Discov.*, **3**, 205 (2004);
   https://doi.org/10.1038/nrd1330
7. J.S. Yang, C.S. Lin and C.Y. Hwang, *Org. Lett.*, **3**, 889 (2001);
   https://doi.org/10.1021/ol015524y
8. C.W. Yu, Y.Y. Wen, X.X. Qin and J. Zhang, *Anal. Methods*, **6**, 9825 (2014);
   https://doi.org/10.1039/C4AY01863J
9. M. Ghaedi, F. Ahmadi and A. Shokrollahi, *J. Hazard. Mater.*, **142**, 272 (2007);
   https://doi.org/10.1016/j.jhazmat.2006.08.012
10. S.M. Xu, Y.L. Liu, H. Yang, K. Zhao, J. Li and A. Deng, *Anal. Chim. Acta*, **964**, 150 (2017);
    https://doi.org/10.1016/j.aca.2017.01.037
11. L. Liu and H. Lin, *Anal. Chem.*, **86**, 8829 (2014);
    https://doi.org/10.1021/ac5021886
12. D. Sarkar, A.K. Pramanik and T.K. Mondal, *RSC Adv.*, **4**, 25341 (2014);
    https://doi.org/10.1039/C4RA02765E
13. O.A. Egorova, H. Seo, A. Chatterjee and K.H. Ahn, *Org. Lett.*, **12**, 401 (2010);
    https://doi.org/10.1021/ol902395x
14. M. Adamczyk and J. Grote, *Synth. Commun.*, **31**, 2681 (2001);
    https://doi.org/10.1081/SCC-100105396
15. J.B. Grimm and L.D. Lavis, *Org. Lett.*, **13**, 6354 (2011);
    https://doi.org/10.1021/ol202618t
16. M. Rajasekar, *J. Mol. Struct.*, **1224**, 129085 (2021);
    https://doi.org/10.1016/j.molstruc.2020.129085
17. H. Zheng, X.Q. Zhan, Q.N. Bian and X.J. Zhang, *Chem. Commun.*, **49**, 429 (2013);
    https://doi.org/10.1039/C2CC35997A
18. G. Shabir, A. Saeed and P.A. Channar, *Mini Rev. Org. Chem.*, **15**, 166 (2018);
    https://doi.org/10.2174/1570193X14666170518130008
19. E. Pérez-Botella, S. Valencia and F. Rey, *Chem. Rev.*, **122**, 17647 (2022);
    https://doi.org/10.1021/acs.chemrev.2c00140
20. P. Li, T. Zhao and H. Li, *Mikrochim. Acta*, **184**, 4663 (2017);
    https://doi.org/10.1007/s00604-017-2501-z
21. I. Pellejero, M. Urbiztondo, D. Izquierdo, S. Irusta, I. Salinas and M.P. Pina, *Ind. Eng. Chem. Res.*, **46**, 2335 (2007);
    https://doi.org/10.1021/ie061025v
22. D. Viboonratanasri, S. Pabchanda and P. Prompinit, *Appl. Surf. Sci.*, **440**, 1261 (2018);
    https://doi.org/10.1016/j.apsusc.2018.01.156
23. A.R. Bertão, N. Pires, A.M. Fonseca, O.S.G.P. Soares, M.F.R. Pereira, T. Dong and I.C. Neves, *Sens. Actuators B Chem.*, **261**, 66 (2018);
    https://doi.org/10.1016/j.snb.2018.01.071
24. X. Wang, H. Guo, N. Wu, M. Xu, L. Zhang and W. Yang, *Colloids Surf. A Physicochem. Eng. Asp.*, **615**, 126218 (2021);
    https://doi.org/10.1016/j.colsurfa.2021.126218
25. I.R. Saragi, Y.K. Krisnandi and R. Sihombing, *Mater. Today Proc.*, **13**, 76 (2018);
    https://doi.org/10.1016/j.matpr.2019.03.191
26. T. Li, Z. Yang, Y. Li, Z. Liu, G. Qi and B. Wang, *Dyes Pigments*, **88**, 103 (2011);
    https://doi.org/10.1016/j.dyepig.2010.05.008
27. I.C. Neves, C. Cunha, R. Pereira, M.F.R. Pereira and A.M. Fonseca, *J. Phys. Chem. C*, **114**, 10719 (2010);
    https://doi.org/10.1021/jp101001a
28. R.A. De Toledo, M.C. Santos, E.T.G. Cavalheiro and L.H. Mazo, *Anal. Bioanal. Chem.*, **381**, 1161 (2005);
    https://doi.org/10.1007/s00216-005-3066-y
29. S. Hashimoto, H.R. Moon and K.B. Yoon, *Micropor. Mesopor. Mater.*, **101**, 10 (2007);
    https://doi.org/10.1016/j.micromeso.2006.12.010
30. M. Zendehdel, A. Babaei and S.J. Alami, *Incl. Phenom. Macrocycl. Chem.*, **59**, 345 (2007);
    https://doi.org/10.1007/s10847-007-9334-z
31. D. Vu, M. Marquez and G. Larsen, *Micropor. Mesopor. Mater.*, **55**, 93 (2002);
    https://doi.org/10.1016/S1387-1811(02)00409-2
32. A. Datt, E.A. Burns, N.A. Dhuna and S.C. Larsen, *Micropor. Mesopor. Mater.*, **167**, 182 (2013);
    https://doi.org/10.1016/j.micromeso.2012.09.011
33. X. Lai, R. Wang, J. Li, G. Qiu and J.B. Liu, *RSC Adv.*, **9**, 22053 (2019);
    https://doi.org/10.1039/C9RA03776D